

Non Uniform Rational Basis Splines (NURBS) is a mathematical representation of a geometry in 3D used for curves and surfaces.

NURBS representation is widely used in Computer-aided design (CAD) to create and modify designs offering smooth surfaces. Due to the success of the use of NURBS in CAD, it has been suggested in other applications. An example of this is the isogeometric analysis introduced by Hughes et al. [69], which is a new method to solve problems governed by partial differential equations such as, structures and fluids. This method has many features in common with the finite element method and some in common with meshless methods. However, it is more geometrically based and takes inspiration from Computer Aided Design (CAD).

Kiendl et al. [70] reports that in isogeometric analysis the functions from the geometry description are used as basis functions for the analysis. Thus, the analysis works on a geometrically exact model and no meshing is necessary. This offers a possibility to close the existing gap between design and analysis as both use the same geometry model.

Another application of NURBS in numerical analysis is the NURBS-enhanced finite element method (NEFEM). Sevilla et al. [71] reports that the NEFEM uses NURBS to accurately describe the boundary of the computational domain, but it differs from isogeometric methods in two main facts. First, NURBS are used to describe the boundary of the computational domain, not the entire domain as done in isogeometric methods. Second, the solution is approximated using polynomials and the approximation is defined with Cartesian coordinates, directly in the physical space. From a practical point of view, NEFEM considers efficient strategies for numerical integration on elements affected by curved boundaries.

The proposed NURBS application is for constitutive material modeling. NURBS surfaces are used to represent the interaction between stresses and strains, i.e., the NURBS surfaces are used here as response surfaces. These NURBS surfaces are based on two axes of strain and one axis of stress. NURBS curves can also be used with one axis of strain and one axis of stress. The constitutive material tensor is calculated with the derivatives from the NURBS surfaces and curves.

To the author knowledge, the only reference to the use of NURBS as response surface for the proposed material model is the linear elastic plane stress material model based on NURBS (LE-NURBS) implemented in CARAT++ by A. Widhammer [51]. This material model consists of two NURBS surfaces and one curve.

The material model based on NURBS for principal directions (PD-NURBS) is a model for materials using stress and strain in principal directions.

4.1

Nonuniform rational B-Spline curves and surfaces

The concept of NURBS curve and surface used in the present study refers to the works of Piegl and Tiller [72] and L. Piegl [73].

The definition of NURBS curve/surface is the rational generalization of the tensor-product nonrational B-spline curve/surface. Therefore the concepts of tensor-product surfaces and B-spline curve/surface will be introduced.

According to Rogers [74], technically, a NURBS surface is a special case of a general rational B-spline surface that uses a particular form of knot vector. For a NURBS surface, the knot vector has multiplicity of duplicate knot values equal to the order of the basis function at the ends. The knot vector may or may not have uniform internal knot values.

4.1.1

Tensor product surfaces

The curve $C(u)$ is a vector-valued function of one parameter. It is a mapping of a straight line segment into Euclidean three-dimensional space. A surface is a vector-valued function of two parameters, u and v , and represents a mapping of a region, of the uv plane into Euclidean three-dimensional space. Thus it has the form $S(u, v) = (x(u, v), y(u, v), z(u, v))$.

The tensor product method is basically a bidirectional curve scheme. It uses basis functions and geometric coefficients. The basis functions are bivariate functions of u and v , which are constructed as products of univariate basis functions. The geometric coefficients are arranged in a bidirectional, $n \times m$ net. Thus, a tensor product surface has the form:

$$S(u, v) = (x(u, v), y(u, v), z(u, v)) = \sum_{i=0}^n \sum_{j=0}^m f_i(u)g_j(v)\mathbf{b}_{i,j} \quad (4-1)$$

where $\mathbf{b}_{i,j} = (x_{i,j}, y_{i,j}, z_{i,j})$, $0 \leq u$, and $v \leq 1$

$S(u, v)$ can be rewritten in matrix form:

$$S(u, v) = [f_i(u)]^T [\mathbf{b}_{i,j}] [g_j(v)] \quad (4-2)$$

where $[f_i(u)]^T$ is a $(1) \times (n+1)$ row vector, $[g_j(v)]$ is a $(m+1) \times (1)$ column vector, and $[b_{i,j}]$ is a $(n+1) \times (m+1)$ matrix of three-dimensional points.

4.1.2

Definition of B-spline basis functions

Let $U = \{u_0, \dots, u_m\}$ be a nondecreasing sequence of real numbers, i.e., $u_i \leq u_{i+1}, i = 0, \dots, m-1$. The u_i are called knots, and U is the knot vector. The i th B-spline basis functions of p -degree (order $p+1$), denoted by $N_{i,p}(u)$, are defined as

$$N_{i,0}(u) = \begin{cases} 1 & \text{if } u_i \leq u < u_{i+1} \\ 0 & \text{otherwise} \end{cases} \quad (4-3)$$

$$N_{i,p}(u) = \frac{u - u_i}{u_{i+p} - u_i} N_{i,p-1}(u) + \frac{u_{i+p+1} - u}{u_{i+p+1} - u_{i+1}} N_{i+1,p-1}(u) \quad (4-4)$$

$N_{i,p}$ is written instead of $N_{i,p}(u)$ for brevity.

The derivative of B-spline basis functions is given by:

$$N'_{i,p} = \frac{p}{u_{i+p} - u_i} N_{i,p-1}(u) - \frac{p}{u_{i+p+1} - u_{i+1}} N_{i+1,p-1}(u) \quad (4-5)$$

The proof of equation 4-5 is presented in Piegl and Tiller [72].

4.1.3

Definition of B-spline curves

A p -degree B-spline is defined by

$$C(u) = \sum_{i=0}^n N_{i,p}(u) \mathbf{CP}_i \quad a \leq u \leq b \quad (4-6)$$

where the \mathbf{CP}_i are the control points and the $N_{i,p}(u)$ are the p th-degree B-spline basis functions (equation 4-3) defined on the nonperiodic and nonuniform knot vector

$$U = \{\underbrace{a, \dots, a}_{p+1}, u_{p+1}, \dots, u_{m-p-1}, \underbrace{b, \dots, b}_{p+1}\} \quad (4-7)$$

with $n + 1$ number of control points and $m + 1$ number of knots are related by:

$$m = n + p + 1 \quad (4-8)$$

The derivative of B-spline curve is given by:

$$C'(u) = \sum_{i=0}^n N'_{i,p}(u) \mathbf{CP}_i \quad (4-9)$$

Substituting equation 4-5 in equation 4-9

$$\begin{aligned} C'(u) &= \sum_{i=0}^n \left(\frac{p}{u_{i+p}-u_i} N_{i,p-1}(u) - \frac{p}{u_{i+p+1}-u_{i+1}} N_{i+1,p-1}(u) \right) \mathbf{CP}_i \\ &= p \sum_{i=0}^{n-1} N_{i+1,p-1}(u) \frac{\mathbf{CP}_{i+1}}{u_{i+p+1}-u_{i+1}} - p \sum_{i=0}^n N_{i+1,p-1}(u) \frac{\mathbf{CP}_i}{u_{i+p+1}-u_{i+1}} \\ &= p \frac{N_{0,p-1}(u) \mathbf{CP}_0}{u_p-u_0} + p \sum_{i=0}^{n-1} N_{i+1,p-1}(u) \frac{\mathbf{CP}_{i+1}-\mathbf{CP}_i}{u_{i+p+1}-u_{i+1}} - p \frac{N_{n+1,p-1}(u) \mathbf{CP}_n}{u_{n+p+1}-u_{n+1}} \end{aligned} \quad (4-10)$$

The first and last terms yield the quotient $\frac{0}{0}$, which is here set zero. Thus equation 4-10 results:

$$C'(u) = \sum_{i=0}^{n-1} N_{i+1,p-1}(u) \frac{\mathbf{CP}_{i+1}-\mathbf{CP}_i}{u_{i+p+1}-u_{i+1}} = \sum_{i=0}^{n-1} N_{i+1,p-1}(u) \mathbf{Q}_i \quad (4-11)$$

where $\mathbf{Q}_i = \frac{\mathbf{CP}_{i+1}-\mathbf{CP}_i}{u_{i+p+1}-u_{i+1}}$.

Considering U' the knot obtained by dropping the first and last knots from U :

$$U' = \{\underbrace{a, \dots, a}_p, u_{p+1}, \dots, u_{m-p-1}, \underbrace{b, \dots, b}_p\} \quad (4-12)$$

it has $m-1$ knots. Then it is easy to check that the function $N_{i+1,p-1}(u)$, computed on U , is equal to $N_{i,p-1}(u)$ computed on U' . Thus

$$C'(u) = \sum_{i=0}^{n-1} N_{i,p-1}(u) \mathbf{Q}_i \quad (4-13)$$

and $C'(u)$ is a $p-1$ th-degree B-spline curve.

4.1.4

Definition of B-spline surfaces

Taking a bidirectional net of control points, two knot vectors, and the products of the univariate B-spline functions a B-spline surface is defined as:

$$S(u, v) = \sum_{i=0}^n \sum_{j=0}^m N_{i,p}(u) N_{j,q}(v) \mathbf{CP}_{i,j} \quad (4-14)$$

with

$$U = \{\underbrace{0, \dots, 0}_{p+1}, u_{p+1}, \dots, u_{r-p-1}, \underbrace{1, \dots, 1}_{p+1}\}$$

$$V = \underbrace{\{0, \dots, 0\}}_{q+1}, \dots, u_{q+1}, \dots, u_{s-q-1}, \underbrace{1, \dots, 1}_{q+1}$$

The knot vector U has $r + 1$ knots, and knot vector V has $s + 1$ knots. Equation 4-8 takes the form

$$r = n + p + 1 \quad \text{and} \quad s = m + q + 1 \quad (4-15)$$

Figure 4.1 shows an example of a B-spline surface.

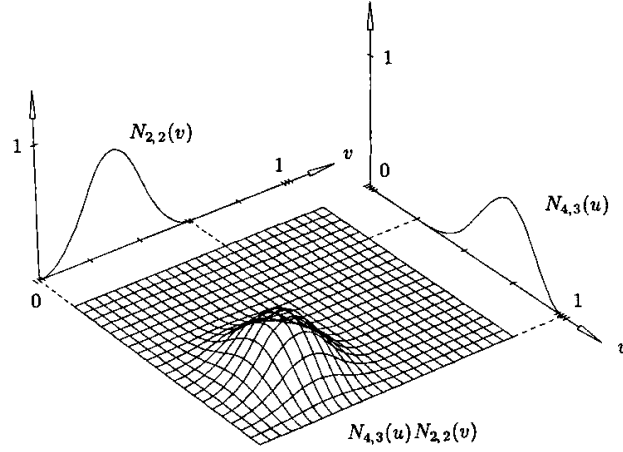


Figure 4.1: Example of a B-spline surface (source: Piegl and Tiller [73])

The derivative of a B-spline surface w.r.t. u is given by

$$\begin{aligned} S_u(u, v) &= \frac{\partial S(u, v)}{\partial u} = \sum_{j=0}^m N_{j,q}(v) \frac{\partial \sum_{i=0}^n N_{i,p}(u) \mathbf{CP}_{i,j}}{\partial u} \\ &= \sum_{j=0}^m N_{j,q}(v) \frac{\partial C_j(u)}{\partial u} \end{aligned} \quad (4-16)$$

where $C_j(u) = \sum_{i=0}^n N_{i,p}(u) \mathbf{CP}_{i,j}$ $j = 0, \dots, m$ are B-spline curves. Applying equation 4-13 into equation 4-16 gives

$$S_u(u, v) = \sum_{i=0}^{n-1} \sum_{j=0}^m N_{i,p-1}(u) N_{j,q}(v) \mathbf{CP}_{i,j}^{(1,0)} \quad (4-17)$$

where

$$\begin{aligned} \mathbf{CP}_{i,j}^{(1,0)} &= \frac{\mathbf{CP}_{i+1,j} - \mathbf{CP}_{i,j}}{u_{i+p+1} - u_{i+1}} \\ U^{(1)} &= \underbrace{\{a, \dots, a\}}_p, u_{p+1}, \dots, u_{r-p-1}, \underbrace{\{b, \dots, b\}}_p \\ V^{(0)} &= V \end{aligned}$$

Analogously $S_v(u, v)$ is given by:

$$S_v(u, v) = \sum_{i=0}^n \sum_{j=0}^{m-1} N_{i,p}(u) N_{j,q-1}(v) \mathbf{CP}_{i,j}^{(0,1)} \quad (4-18)$$

where

$$\mathbf{CP}_{i,j}^{(0,1)} = \frac{\mathbf{CP}_{i,j+1} - \mathbf{CP}_{i,j}}{v_{j+q+1} - v_{j+1}}$$

$$U^{(0)} = U$$

$$V^{(1)} = \{\underbrace{a, \dots, a}_q, v_{q+1}, \dots, v_{s-q-1}, \underbrace{b, \dots, b}_q\}$$

4.1.5

Definition of NURBS curves

Based in the previous definitions, a p th-degree NURBS curve is defined by:

$$C^{NURBS}(u) = \frac{\sum_{i=0}^n w_i \mathbf{CP}_i N_{i,p}(u)}{\sum_{i=0}^n w_i N_{i,p}(u)} \quad a \leq u \leq b \quad (4-19)$$

where w_i are the weights, \mathbf{CP}_i are the control points that form a control polygon, and $N_{i,p}(u)$ are the normalized B-splines of degree p in u direction, defined over the knot vector \mathbf{U}^{NURBS} .

$$U^{NURBS} = [\underbrace{a, \dots, a}_{p+1}, u_{p+1}, \dots, u_{m-p-1}, \underbrace{b, \dots, b}_{p+1}] \quad (4-20)$$

We assume that $a = 0$, $b = 1$, and $w_i > 0$ for all i . Setting:

$$R_{i,p}(u) = \frac{N_{i,p}(u) w_i}{\sum_{j=0}^n N_{j,p}(u) w_j} \quad (4-21)$$

equation 4-19 is rewritten in the form:

$$C^{NURBS}(u) = \sum_{i=0}^n R_{i,p}(u) \mathbf{CP}_i \quad (4-22)$$

$R_{i,p}(u)$ are the rational basis functions.

For the properties of NURBS curves, we refer to Piegl and Tiller [72]. Figure 4.2 illustrates the construction of a NURBS curve.

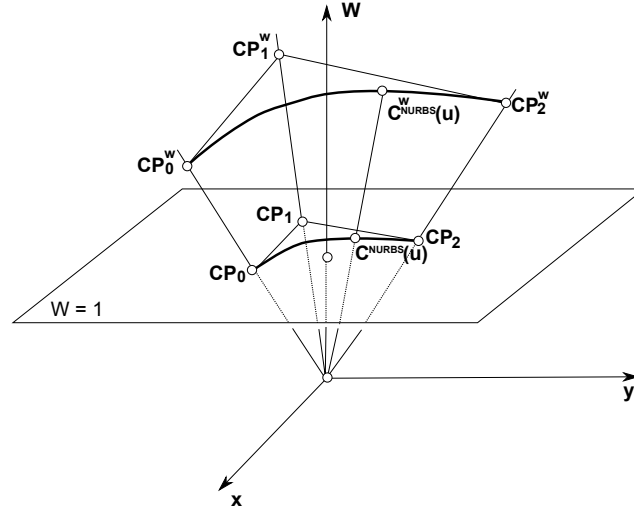


Figure 4.2: Geometry construction of a NURBS curve (source: Piegl and Tiller [73])

4.1.6

Derivatives of a NURBS curve

The derivatives of NURBS curve are computed with the derivatives of nonrational B-spline curves. Considering $C^{NURBS}(u)$ as follows:

$$C^{NURBS}(u) = \frac{w(u)C^{NURBS}(u)}{w(u)} = \frac{A(u)}{w(u)} \quad (4-23)$$

where $A(u)$ is the numerator of equation 4-19. Differentiating equation 4-23, results:

$$\begin{aligned} C^{NURBS'}(u) &= \frac{w(u)A'(u) - w'(u)A(u)}{w(u)^2} \\ &= \frac{w(u)A'(u) - w'(u)w(u)C(u)}{w(u)^2} = \frac{A'(u) - w'(u)C(u)}{w(u)} \end{aligned} \quad (4-24)$$

where

$$A'(u) = \sum_{i=0}^n w_i \mathbf{CP}_i N'_{i,p}(u) \quad (4-25)$$

$$w'_i(u) = \sum_{i=0}^n w_i N'_{i,p}(u) \quad (4-26)$$

and $N'_{i,p}(u)$ is given by equation 4-5

4.1.7

Definition of NURBS surfaces

A NURBS surface is a bivariate vector-valued piecewise rational function of the form

$$S^{NURBS}(u, v) = \frac{\sum_{i=0}^n \sum_{j=0}^m w_{i,j} \mathbf{CP}_{i,j} N_{i,p}(u) N_{j,q}(v)}{\sum_{i=0}^n \sum_{j=0}^m w_{i,j} N_{i,p}(u) N_{j,q}(v)} \quad 0 \leq u, v \leq 1 \quad (4-27)$$

where $w_{i,j}$ are the weights, $\mathbf{CP}_{i,j}$ are the control points that form a control net, and $N_{i,p}(u)$ and $N_{j,q}(v)$ are the nonrational B-spline basis functions of degree p and q in the u and v directions, respectively, defined over the knot vectors:

$$U^{NURBS} = [\underbrace{0, \dots, 0}_{p+1}, u_{p+1}, \dots, u_{r-p-1}, \underbrace{1, \dots, 1}_{p+1}] \quad (4-28)$$

$$V^{NURBS} = [\underbrace{0, \dots, 0}_{q+1}, v_{q+1}, \dots, v_{s-q-1}, \underbrace{1, \dots, 1}_{q+1}] \quad (4-29)$$

where $r = n + p + 1$ and $s = m + q + 1$.

Introducing the piecewise rational basis functions:

$$R_{i,j}(u, v) = \frac{N_{i,p}(u) N_{j,q}(v) w_{i,j}}{\sum_{k=0}^n \sum_{l=0}^m N_{k,p}(u) N_{l,q}(v) w_{k,l}} \quad (4-30)$$

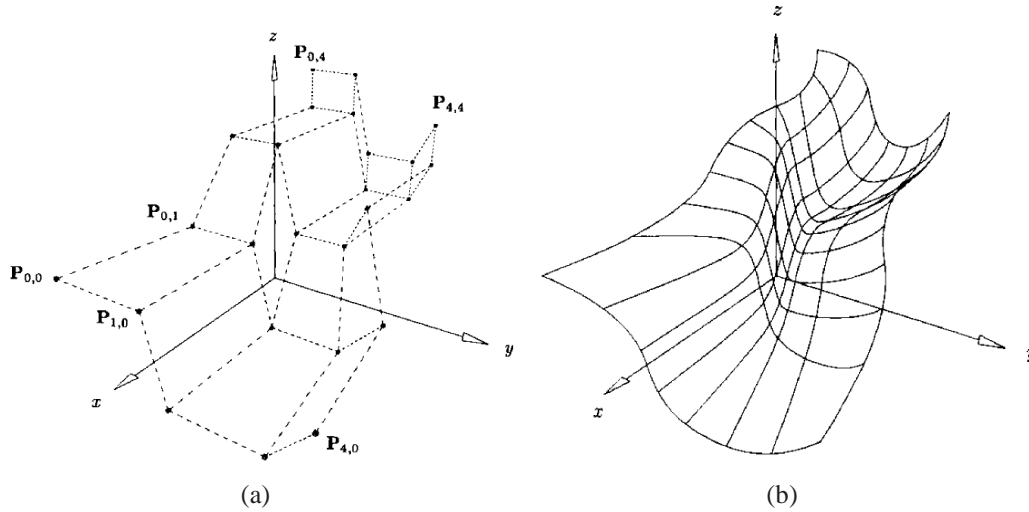


Figure 4.3: NURBS surface: (a) Control points net (b) biquadratic NURBS surface (source: Piegl and Tiller [72])

Equation 4-27 is rewritten as

$$S^{NURBS}(u, v) = \sum_{i=0}^n \sum_{j=0}^m R_{i,j}(u, v) \mathbf{CP}_{i,j} \quad (4-31)$$

A NURBS surface example is shown in figure 4.3

4.1.8

Derivatives of a NURBS surface

The derivatives of a NURBS surface are computed analogously to the derivatives of a NURBS curve. Considering $S^{NURBS}(u, v)$ as follows:

$$S^{NURBS}(u, v) = \frac{w(u, v)S^{NURBS}(u, v)}{w(u, v)} = \frac{A(u, v)}{w(u, v)} \quad (4-32)$$

where $A(u, v)$ is the numerator of equation 4-27, the derivatives of a NURBS surface are calculated:

$$S_{\alpha}^{NURBS}(u, v) = \frac{A_{\alpha}(u, v) - w_{\alpha}(u, v)S^{NURBS}(u, v)}{w(u, v)} \quad (4-33)$$

and α denotes either u or v . In the above expression $A_{\alpha}(u, v)$ is given by:

$$\begin{aligned} A_{\alpha}(u, v) &= w(u, v) \frac{\partial}{\partial \alpha} S^{NURBS}(u, v) \\ &= w(u, v) \left(\frac{\partial}{\partial \alpha} \sum_{j=0}^m N_{j,q}(v) \sum_{i=0}^n N_{i,p}(u) \mathbf{CP}_{i,j} \right) \end{aligned} \quad (4-34)$$

The final expressions for the derivatives of a NURBS surface in direction u follow:

$$\begin{aligned} \frac{\partial}{\partial u} \sum_{i=0}^n N_{i,p}(u) \mathbf{CP}_{i,j} &= \sum_{i=0}^{n-1} N_{i,p-1}(u) \mathbf{CP}_{i,j}^{(1,0)} \\ S_u^{NURBS}(u, v) &= \sum_{i=0}^{n-1} \sum_{j=0}^m N_{i,p-1}(u) N_{j,q}(v) \mathbf{CP}_{i,j}^{(1,0)} \end{aligned} \quad (4-35)$$

where

$$\begin{aligned} \mathbf{CP}_{i,j}^{(1,0)} &= p \frac{\mathbf{CP}_{i+1,j} - \mathbf{CP}_{i,j}}{u_{i+p+1} - u_{i+1}} \\ U^{NURBS(1)} &= [\underbrace{0, \dots, 0}_p, u_{p+1}, \dots, u_{r-p-1}, \underbrace{1, \dots, 1}_p] \\ V^{NURBS(0)} &= V^{NURBS} \end{aligned}$$

Analogously for direction v :

$$S_v^{NURBS}(u, v) = \sum_{i=0}^n \sum_{j=0}^{m-1} N_{i,p}(u) N_{j,q-1}(v) \mathbf{CP}_{i,j}^{(0,1)} \quad (4-36)$$

where

$$\mathbf{CP}_{i,j}^{(0,1)} = q \frac{\mathbf{CP}_{i,j+1} - \mathbf{CP}_{i,j}}{v_{j+q+1} - v_{j+1}}$$

$$\mathbf{U}^{NURBS^{(0)}} = \mathbf{U}^{NURBS}$$

$$\mathbf{V}^{NURBS^{(1)}} = [\underbrace{0, \dots, 0}_q, v_{q+1}, \dots, v_{s-q-1}, \underbrace{1, \dots, 1}_q]$$

4.2

Linear elastic material model based on NURBS (LE–NURBS)

This material model was developed by A. Widhammer [51].

Considering the plane stress condition the stress and strain tensors are given by equations 4-37 and 4-38, respectively.

$$\mathbf{S} = \begin{bmatrix} S_{11} & S_{22} & S_{12} \end{bmatrix} \quad (4-37)$$

$$\mathbf{E} = \begin{bmatrix} E_{11} & E_{22} & 2E_{12} \end{bmatrix} \quad (4-38)$$

Two NURBS surfaces are defined: one for the stress S_{11} and the other for the stress S_{22} with the common strain axes E_{11} and E_{22} . Additionally the NURBS curve is defined with the shear strain (E_{12}) in one axis and the shear stress (S_{12}) in the other. Illustration of the LE–NURBS surfaces and curve are presented in figure 4.4. Because of the model linearity, the surfaces are flat and the curve is linear.

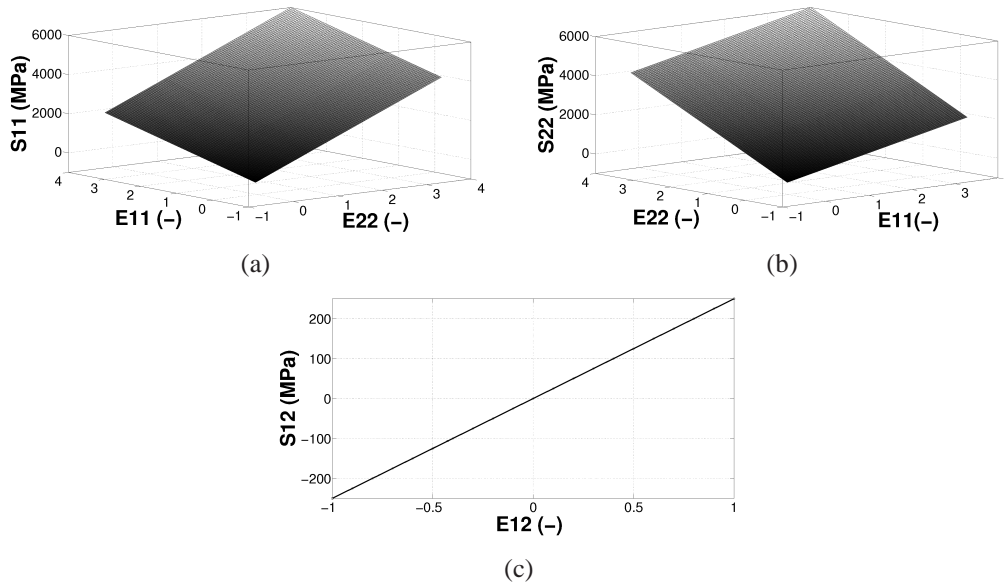


Figure 4.4: NURBS surfaces for stresses and strains for LE–NURBS material: (a) stresses in direction 11 and strains in directions 11 and 22, (b) stresses in direction 22 and strains in directions 11 and 22 and, (c) NURBS curve for stresses in direction 12 and strains in direction 12.

For given strain input values the corresponding stresses are obtained on the NURBS surfaces.

The LE-NURBS constitutive material tensor presented in equation 4-39 is given by the derivatives: $\frac{dS_{11}}{dE_{11}}$, $\frac{dS_{11}}{dE_{22}}$, $\frac{dS_{22}}{dE_{11}}$, $\frac{dS_{22}}{dE_{22}}$ and $\frac{dS_{12}}{2dE_{12}}$, which are the derivatives of the NURBS surfaces and curve. These derivatives are calculated following the NURBS theory presented in section 4.1.

$$\frac{d\mathbf{S}}{d\mathbf{E}} = \begin{bmatrix} \frac{dS_{11}}{dE_{11}} & \frac{dS_{11}}{dE_{22}} & 0 \\ \frac{dS_{22}}{dE_{11}} & \frac{dS_{22}}{dE_{22}} & 0 \\ 0 & 0 & \frac{dS_{12}}{2dE_{12}} \end{bmatrix} \quad (4-39)$$

where

$$\begin{bmatrix} \frac{dS_{11}}{dE_{11}} \\ \frac{dS_{11}}{dE_{22}} \end{bmatrix} = \left(\begin{bmatrix} \frac{dE_{11}}{du} & \frac{dE_{22}}{du} \\ \frac{dE_{11}}{dv} & \frac{dE_{22}}{dv} \end{bmatrix} \right)^{-T} \cdot \begin{bmatrix} \frac{dS_{11}}{du} \\ \frac{dS_{11}}{dv} \end{bmatrix} \quad (4-40)$$

$$\begin{bmatrix} \frac{dS_{22}}{dE_{11}} \\ \frac{dS_{22}}{dE_{22}} \end{bmatrix} = \left(\begin{bmatrix} \frac{dE_{11}}{du} & \frac{dE_{22}}{du} \\ \frac{dE_{11}}{dv} & \frac{dE_{22}}{dv} \end{bmatrix} \right)^{-T} \cdot \begin{bmatrix} \frac{dS_{22}}{du} \\ \frac{dS_{22}}{dv} \end{bmatrix} \quad (4-41)$$

$$\frac{dS_{12}}{dE_{12}} = \frac{dS_{12}}{du} \cdot \left(\frac{dE_{12}}{du} \right)^{-1} \quad (4-42)$$

The derivatives of the NURBS surface for S_{11} in directions u and v are given by

$$S_{u11}^{NURBS}(u, v) = \left[\frac{dE_{11}}{du} \quad \frac{dE_{22}}{du} \quad \frac{dS_{11}}{du} \right] \quad (4-43)$$

$$S_{v11}^{NURBS}(u, v) = \left[\frac{dE_{11}}{dv} \quad \frac{dE_{22}}{dv} \quad \frac{dS_{11}}{dv} \right] \quad (4-44)$$

and analogously for the derivatives of the NURBS surface for S_{22} in directions u and v .

$$S_{u22}^{NURBS}(u, v) = \left[\frac{dE_{11}}{du} \quad \frac{dE_{22}}{du} \quad \frac{dS_{22}}{du} \right] \quad (4-45)$$

$$S_{v22}^{NURBS}(u, v) = \left[\frac{dE_{11}}{dv} \quad \frac{dE_{22}}{dv} \quad \frac{dS_{22}}{dv} \right] \quad (4-46)$$

The derivative of the NURBS curve for stress S_{12} in direction u is

$$C^{NURBS'}(u) = \left[\frac{dE_{12}}{du} \quad \frac{dS_{12}}{du} \right] \quad (4-47)$$

4.3

Material model based on NURBS for principal directions (PD-NURBS)

The proposed material model covers isotropic nonlinear materials under plane stress conditions, consequently the LE-NURBS is also included. The principal difference between this model and the LE-NURBS material model is that the PD-

NURBS is based on principal directions of stress and strain. Therefore only one surface is required for its definition.

PD-NURBS is valid for isotropic materials because of the use of orthogonal transformation to calculate the response of the stress. According to Gruttmann and Taylor [60], for isotropic material response the contravariant components of the Second Piola–Kirchhoff stress tensor are recovered by an orthogonal transformation of the principal stresses.

The second Piola–Kirchhoff stresses and the Green–Lagrange strains in principal directions are given by:

$$\hat{\mathbf{S}} = \begin{bmatrix} S_1 & S_2 & \hat{S}_{12} \end{bmatrix} \quad (4-48)$$

$$\hat{\mathbf{E}} = \begin{bmatrix} E_1 & E_2 & \hat{E}_{12} \end{bmatrix} \quad (4-49)$$

where $\hat{S}_{12} = 0$ and $\hat{E}_{12} = 0$.

The constitutive material tensor in general directions is obtained with the rotation matrix calculated as follows:

$$\frac{d\mathbf{S}}{d\mathbf{E}} = \begin{bmatrix} \frac{dS_{11}}{dE_{11}} & \frac{dS_{11}}{dE_{22}} & \frac{dS_{11}}{2d\hat{E}_{12}} \\ \frac{dS_{22}}{dE_{11}} & \frac{dS_{22}}{dE_{22}} & \frac{dS_{22}}{2d\hat{E}_{12}} \\ \frac{dS_{12}}{dE_{11}} & \frac{dS_{12}}{dE_{22}} & \frac{dS_{12}}{2d\hat{E}_{12}} \end{bmatrix} = \mathbf{T}^T \cdot \frac{d\hat{\mathbf{S}}}{d\hat{\mathbf{E}}} \cdot \mathbf{T} \quad (4-50)$$

where $\frac{d\hat{\mathbf{S}}}{d\hat{\mathbf{E}}}$ is the constitutive material tensor in principal directions

$$\frac{d\hat{\mathbf{S}}}{d\hat{\mathbf{E}}} = \begin{bmatrix} \frac{dS_1}{dE_1} & \frac{dS_1}{dE_2} & \frac{dS_1}{2d\hat{E}_{12}} \\ \frac{dS_2}{dE_1} & \frac{dS_2}{dE_2} & \frac{dS_2}{2d\hat{E}_{12}} \\ \frac{d\hat{S}_{12}}{dE_1} & \frac{d\hat{S}_{12}}{dE_2} & \frac{d\hat{S}_{12}}{2d\hat{E}_{12}} \end{bmatrix} = \begin{bmatrix} \frac{dS_1}{dE_1} & \frac{dS_1}{dE_2} & 0 \\ \frac{dS_2}{dE_1} & \frac{dS_2}{dE_2} & 0 \\ 0 & 0 & \frac{d\hat{S}_{12}}{2d\hat{E}_{12}} \end{bmatrix} \quad (4-51)$$

and the rotation matrix \mathbf{T} is the same matrix introduced for the Ogden material in chapter 3 section 3.3.3.

$$\mathbf{T} = \begin{bmatrix} \cos^2\phi & \sin^2\phi & \cos\phi\sin\phi \\ \sin^2\phi & \cos^2\phi & -\cos\phi\sin\phi \\ -2\cos\phi\sin\phi & 2\cos\phi\sin\phi & \cos^2\phi - \sin^2\phi \end{bmatrix} \quad (4-52)$$

The constitutive material tensor in principal directions is computed with the

NURBS surface derivatives introduced in section 4.1.8:

$$\begin{bmatrix} \frac{dS_1}{dE_1} \\ \frac{dS_1}{dE_2} \end{bmatrix} = \left(\begin{bmatrix} \frac{dE_1}{du} & \frac{dE_2}{du} \\ \frac{dE_1}{dv} & \frac{dE_2}{dv} \end{bmatrix} \right)^{-T} \cdot \begin{bmatrix} \frac{dS_1}{du} \\ \frac{dS_1}{dv} \end{bmatrix} \quad (4-53)$$

$$\begin{bmatrix} \frac{dS_2}{dE_1} \\ \frac{dS_2}{dE_2} \end{bmatrix} = \left(\begin{bmatrix} \frac{dE_1}{du} & \frac{dE_2}{du} \\ \frac{dE_1}{dv} & \frac{dE_2}{dv} \end{bmatrix} \right)^{-T} \cdot \begin{bmatrix} \frac{dS_2}{du} \\ \frac{dS_2}{dv} \end{bmatrix} \quad (4-54)$$

The derivative $\frac{d\hat{S}_{12}}{2d\hat{E}_{12}}$ is calculated as follows:

$$\mathbf{E} = \frac{1}{2} (\mathbf{F}^T \mathbf{F} - \mathbf{I}) = \frac{1}{2} (\mathbf{C} - \mathbf{I})$$

$$\hat{\mathbf{C}} = \mathbf{T} \cdot \mathbf{C} \quad (4-55)$$

where $\hat{\mathbf{C}}$ and \mathbf{C} are in vector form:

$$\hat{\mathbf{C}} = \begin{bmatrix} \hat{C}_{11} & \hat{C}_{22} & 2\hat{C}_{12} \end{bmatrix} \quad (4-56)$$

$$\mathbf{C} = \begin{bmatrix} C_{11} & C_{22} & 2C_{12} \end{bmatrix} \quad (4-57)$$

Equation 4-55 gives the constraint:

$$\hat{C}_{12} = \hat{C}_{21} = -\frac{1}{2} (C_{11} - C_{22}) \sin(2\phi) + C_{12} \cos(2\phi) = 0 \quad (4-58)$$

$$\mathbf{S} = \mathbf{T}^T \cdot \hat{\mathbf{S}} \quad (4-59)$$

Finally the derivative $\frac{d\hat{S}_{12}}{2d\hat{E}_{12}}$ is calculated with the derivatives $\frac{d\hat{S}_{12}}{d\phi}$ and $\frac{d\phi}{2d\hat{E}_{12}}$ obtained with equation 4-59 and 4-58:

$$\frac{d\hat{S}_{12}}{2d\hat{E}_{12}} = \frac{d\hat{S}_{12}}{d\phi} \cdot \frac{d\phi}{2d\hat{E}_{12}} = \frac{-(S_2 - S_1) \cos 2\phi}{C_{11} - C_{22}} \quad (4-60)$$

where

$$\frac{d\hat{S}_{12}}{d\phi} = \sin \phi \cos \phi (S_{11} - S_{22}) = S_2 - S_1$$

$$\frac{d\phi}{2d\hat{E}_{12}} = \frac{d\phi}{d\hat{C}_{12}} = \frac{-\cos 2\phi}{C_{11} - C_{22}}$$

and C_{11} and C_{22} are the components of the right stretch tensor \mathbf{C} introduced in chapter 2 in section 2.2. The cosine $\cos \phi$ is calculated with the spectral decomposition presented in equations 2-10 and 2-11.

The algorithm of the material model based on NURBS for principal directions

is presented in box 4.1

1. Update the strain tensor.

$$\mathbf{E}_{n+1} = \mathbf{E}_n + \nabla^S u$$

2. Calculate the strains in principal directions

$$\hat{\mathbf{E}}_{n+1} = \mathbf{T}^T \mathbf{E}_{n+1}$$

3. Calculate the local parameter u and v from the strains.

4. Obtain the stress values $S_1(u, v)$, $S_2(u, v)$.

5. Calculate the derivatives $\frac{dS_1}{dE_1}$, $\frac{dS_1}{dE_2}$, $\frac{dS_2}{dE_1}$, $\frac{dS_2}{dE_2}$, and $\frac{d\hat{S}_{12}}{d\hat{E}_{12}}$ (equations 4-53, 4-54 and 4-60).

6. Constitutive material tensor is obtained:

$$\frac{d\mathbf{S}}{d\mathbf{E}} = \mathbf{T}^T \cdot \begin{bmatrix} \frac{dS_1}{dE_1} & \frac{dS_1}{dE_2} & 0 \\ \frac{dS_2}{dE_1} & \frac{dS_2}{dE_2} & 0 \\ 0 & 0 & \frac{d\hat{S}_{12}}{2d\hat{E}_{12}} \end{bmatrix} \cdot \mathbf{T}$$

7. Calculate the stress tensor.

$$\mathbf{S} = \mathbf{T}^T \cdot \hat{\mathbf{S}}$$

Box 4.1: Algorithm of the material model based on NURBS

4.4

Data fitting

Data fitting based on least-squares approximation is used to generate NURBS surfaces for the experimental data. This process is briefly described below. For more details the reference are the work of Piegl and Tiller [73] and L. Piegl [73]. An alternative approach for the generation of NURBS surfaces is the use of a CAD software.

4.4.1

Curve fitting

According to L. Piegl [73] equation 4-22 can be written in matrix form as

$$C^{NURBS} = \mathbf{RCP} \quad (4-61)$$

where C^{NURBS} and \mathbf{CP} are $(n + 1) \times 1$ matrices and \mathbf{R} is an $(n + 1) \times (n + 1)$ matrix. If there are more data points than control points, equation 4-61 is overdetermined and can be solved approximately as follows:

$$C^{NURBS^f} = (\mathbf{R}^T \mathbf{R})^{-1} \mathbf{R}^T \mathbf{CP} \quad (4-62)$$

Assigning initial parameters to the data points, as the p -th degree and the control points, a least-squares fit is generated using equation 4-62.

4.4.2 Surface fitting

The curve-fitting technique can be easily generalized for surfaces yielding:

$$S^{NURBS^f} = (\mathbf{R}^T \mathbf{R})^{-1} \mathbf{R}^T \mathbf{CP} \quad (4-63)$$

4.5 Validation examples

The PD–NURBS material model is applied to examples with different material responses to validate the proposed material model. Attention is given to materials with large strains.

4.5.1 Hyperelasticity — NeoHookean

The hyperelastic example is a quadrilateral membrane with dimensions 1m x 1m and the material properties are shown in table 4.1. For this membrane a finite element model was built for which the mesh, boundary conditions and, loading are presented in figure 4.5. The mesh is composed by 143 nodes and 100 quadrilateral linear elements with 2 x 2 Gauss integration. The load was risen up to 89.44 MN.

Table 4.1: Material properties of quadrilateral membrane example

Young's modulus (E)	250 MPa
Poisson ratio (ν)	0.3
thickness	1 mm

The validation was carried out comparing the solution with a conventional formulation for hyperelastic materials and the nonlinear material model based on

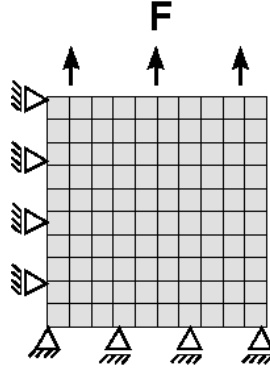
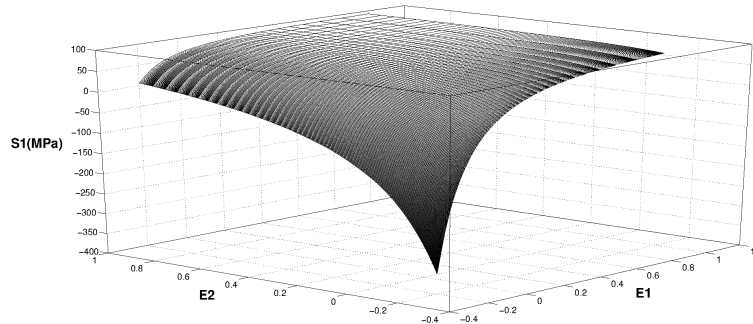


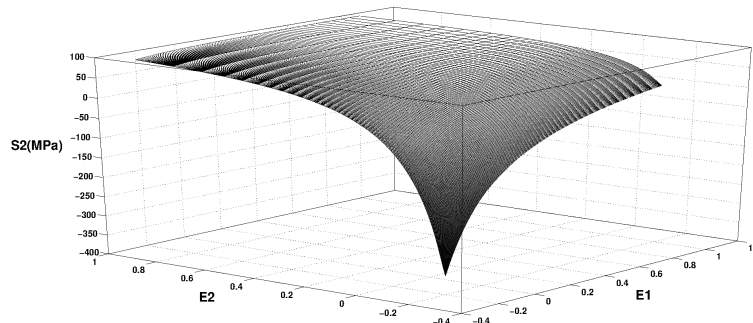
Figure 4.5: Mesh, boundary conditions and applied load for the quadrilateral example

NURBS surfaces. The conventional NeoHookean formulation is obtained with the Ogden material model presented in section 3.3.3 setting: $r = 1$, $\alpha_1 = 2$ and $\mu_1 = G = \frac{E}{2(1+\nu)}$.

Since no experimental data was available for this application, the PD-NURBS surfaces were generated with data points from NeoHookean formulation. The NeoHookean NURBS surfaces are presented in figure 4.6 with stresses and strains in the principal directions. These surfaces are composed by a control point net $25(u) \times 25(v)$ and degree 3 ($p = 3$ and $q = 3$).



(a)



(b)

Figure 4.6: NURBS surfaces of stresses and strains in principal directions for NeoHookean material: (a) stresses in direction 1 and (b) stresses in direction 2.

4.5.1.1 Results

Displacement results in direction y are presented in figure 4.7. The results demonstrate that the solution with the proposed material model is in accordance with the conventional NeoHookean material model formulation.

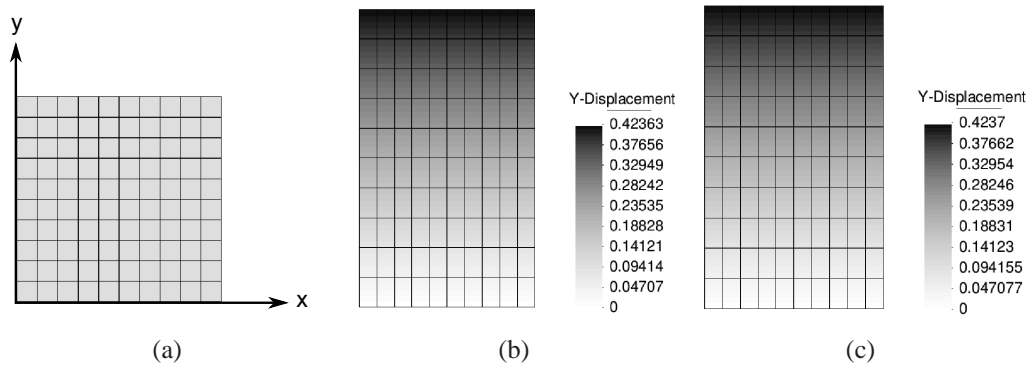


Figure 4.7: Displacement results in y direction: (a) undeformed membrane, (b) conventional material model, and (c) PD-NURBS material model.

The maximum error of the results are shown in Table 4.2 and this is calculated with equation 4-64:

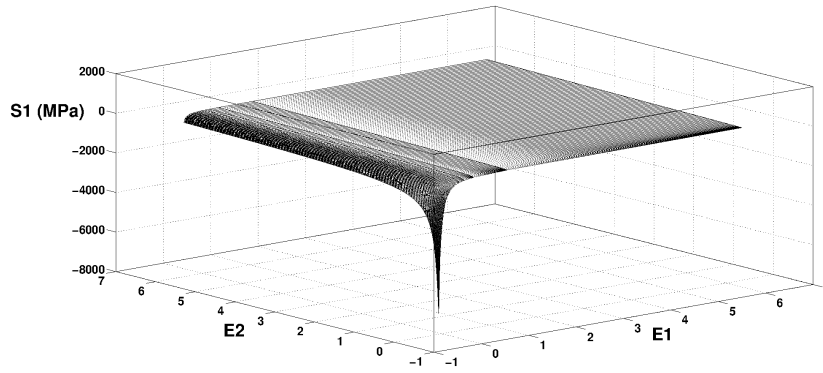
$$Error = \frac{NURBS \text{ result} - Conventional \text{ result}}{Conventional \text{ result}} \cdot 100 \quad (4-64)$$

Table 4.2: Maximum error of the PD-NURBS for rectangular membrane

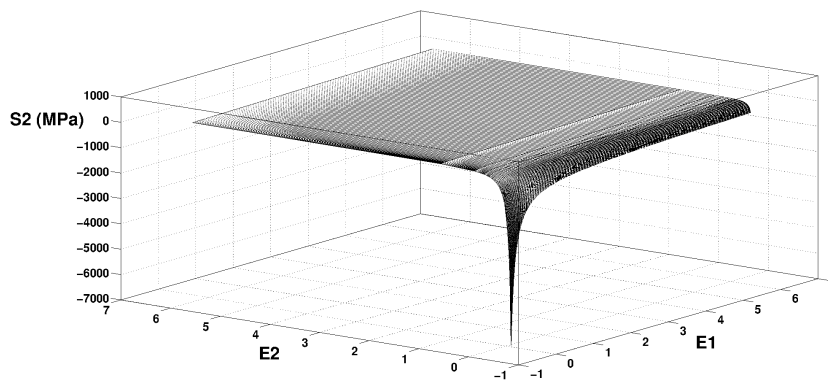
Maximum error	
displacement y	Stress y
0.0165%	0.15%

4.5.2 Hyperelasticity – Mooney-Rivlin

This example was modeled in chapter 3 in section 3.3.4 considering a conventional formulation for Mooney-Rivlin material model. The results obtained before are compared with the nonlinear material model based on NURBS surfaces. Figure 4.8 shows the NURBS surfaces used in these examples. The degree used in the NURBS surfaces is 3 ($p = 3$ and $q = 3$) and the number of control points is increased to analyze the convergence control.



(a)



(b)

Figure 4.8: NURBS surfaces with stresses and strains in principal directions for the Mooney-Rivlin material: (a) stresses in direction 1, and (b) stresses in direction 2.

4.5.2.1 Results

NURBS surfaces are generated for different control point nets. The number of control points are: 15x15, 20x20, 40x40, 70x70, and 100x100. Table 4.3 presents the convergence for each load step comparing the different nets.

For the 15x15 net convergence was achieved by the first step solely. As the number of control points increases the convergence rate increases as well and the number of iterations for each step decreases.

The number of iterations changes substantially for the first two steps comparing the 20x20 and 40x40 nets.

When the number of control points is increased to the 100x100 net the convergence rate is improved for the last step and all the steps have 5 iterations.

Table 4.4 presents the maximum error for the displacement, stress, and strain for the analyzed nets. The error is calculated with equation 4-64 presented in the previous example.

Table 4.3: Displacement residuum for 15x15 to 100x100 control point net.

Step	it.	displacement residuum				
		15x15	20x20	40x40	70x70	100x100
1	1	9.97E+00	1.24E+01	1.14E+01	1.14E+01	1.14E+01
	2	1.67E+00	1.28E+00	1.06E+00	1.05E+00	1.05E+00
	3	1.22E-01	1.21E-01	1.94E-02	2.15E-02	2.14E-02
	4	9.07E-03	1.37E-02	3.08E-04	8.55E-06	1.55E-05
	5	1.43E-03	1.48E-03	4.16E-06	2.23E-09	4.44E-11
	6	1.77E-04	1.65E-04	6.45E-08		
	7	2.81E-05	1.82E-05			
	8	3.92E-06	2.03E-06			
	9	6.05E-07	2.25E-07			
2	1	N.C.	3.18E+01	3.10E+01	7.10E-01	3.10E+01
	2		8.87E+00	7.82E+00	7.95E+00	7.94E+00
	3		7.14E-01	7.07E-01	7.10E-01	7.14E-01
	4		1.67E-01	1.97E-02	2.61E-03	2.13E-03
	5		3.37E-02	1.21E-03	6.57E-06	1.03E-06
	6		9.84E-03	4.68E-05	2.25E-08	2.69E-09
	7		2.29E-03	2.73E-06		
	8		6.54E-04	1.17E-07		
	9		1.64E-04			
	10		4.54E-05			
	11		1.18E-05			
	12		3.20E-06			
	13		8.44E-07			
3	1		4.69E+01	4.84E+01	4.77E+01	4.77E+01
	2		9.71E+00	8.60E+00	8.79E+00	8.78E+00
	3		7.40E-01	2.34E-01	2.58E-01	2.63E-01
	4		1.95E-02	8.72E-03	2.97E-03	2.02E-04
	5		1.37E-03	2.85E-04	7.03E-05	1.81E-07
	6		8.30E-05	3.10E-05	1.05E-06	
	7		7.50E-06	1.17E-06	2.55E-08	
	8		6.27E-07	1.21E-07		

The improvement in the convergence rate observed with the increase in the number of control points, is also observed by the results for displacements, stresses and strains.

The maximum error for the stress in direction $x-x$ has an interesting path as the number of control points increases. The error of 5.558% for the 20x20 control point net, which is quite large, decreases with the number of control points reaching the same results as the conventional material model for the 70x70 control point net. For the 100x100 control point net the value is also the same as the results for conventional material model or the error is very small.

Table 4.4: Maximum error of PD-NURBS material with surfaces generated by control point nets 20x20 to 100x100 for the square perforated example

control points	Maximum error (%)			
	20x20	40x40	70x70	100x100
displacement x	1.341	0.111	0.012	0.000
displacement y	0.264	0.026	0.000	0.000
stress xx	5.558	0.178	0.000	0.010
stress yy	0.489	0.074	0.074	0.011
stress xy	0.859	0.049	0.012	0.006
strain xx	0.743	0.085	0.065	0.011
strain yy	0.400	0.030	0.023	0.003
strain xy	0.445	0.109	0.016	0.000

4.5.3

Comparison with elastoplastic von Mises material model

The von Mises elastoplastic material is used here to investigate the applicability of the PD-NURBS to other stress-strain responses. The example consists in a monotonic stretching of a perforated rectangular membrane modeled in chapter 3 section 3.1.3. The PD-NURBS material is now employed by the constitutive response in the finite element code as presented in box 4.1.

It is worth pointing out that a full elastoplastic stress history can not be obtained with the proposed PD-NURBS since unloading/reloading cycles are not represented by the NURBS surfaces herein.

The membrane material properties are rewritten in table 4.5 and the mesh is composed of 531 nodes and 480 quadrilateral membrane elements with linear discretization and 2 x 2 gauss points integration. The mesh, geometry, boundary conditions, and the applied load are shown in figure 3.4 in section 3.1.3.

Table 4.5: Material properties of the perforated membrane example

Young's modulus (E)	70 GPa
Poisson ratio (ν)	0.2
Yield stress (σ_y)	0.243GPa
Hardening modulus (K)	0.2GPa
thickness	1 mm

The elastoplastic material properties of table 4.5 are used to produce the data points for the generation of the NURBS surfaces in principal directions. These NURBS surfaces are shown in figure 4.9 and they are composed by a control point net 70(u) x 70(v) and degree 2 ($p = 2$ and $q = 2$). The number of control points for the NURBS surfaces is defined with help of the previous example, by which the convergence and maximum error for different control point nets are compared.

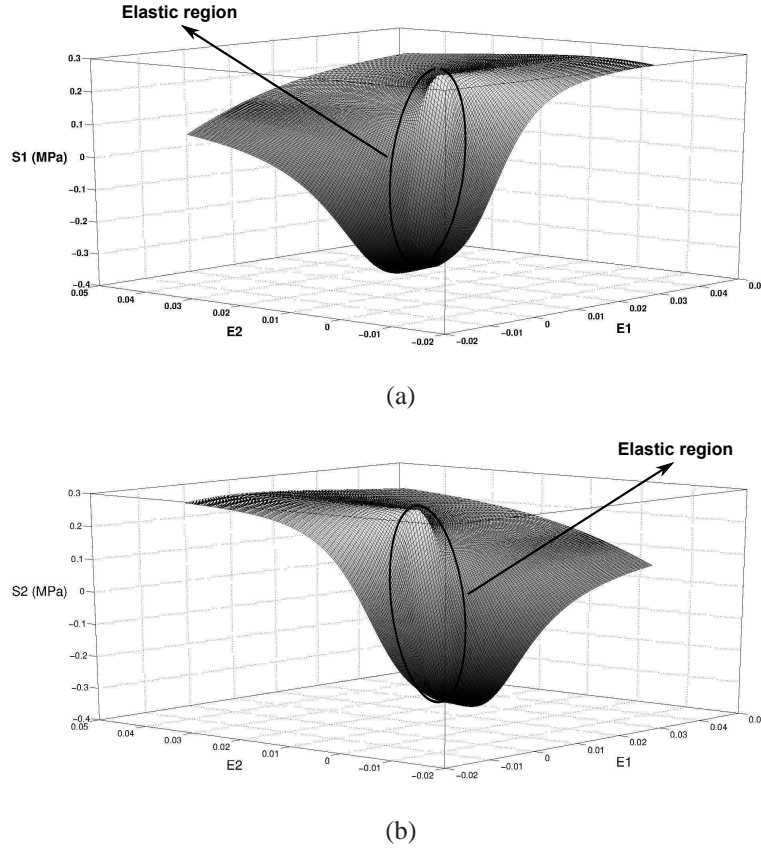


Figure 4.9: NURBS surfaces for stresses and strains in principal directions for elastoplastic material: (a) stresses in direction 1, and (b) stresses in direction 2.

The elastic region can be identified in the NURBS surfaces in Figure 4.9 as the flat ellipse plane. Outside this region nonlinear behavior is presented. Therefore the corresponding axis $S_{11}(u, v)$ and $S_{22}(u, v)$ values fall in the elastoplastic range of the plastic model.

The conventional formulation used for the elastoplastic material model was presented in section 3.1.

4.5.3.1 Results

The results obtained with the PD-NURBS material model are compared with the classical material model. Figures 4.10 and 4.11 show the results for the conventional elastoplastic and the PD-NURBS material model for displacements and stresses in direction y, respectively. The maximum error in the results are shown in table 4.6

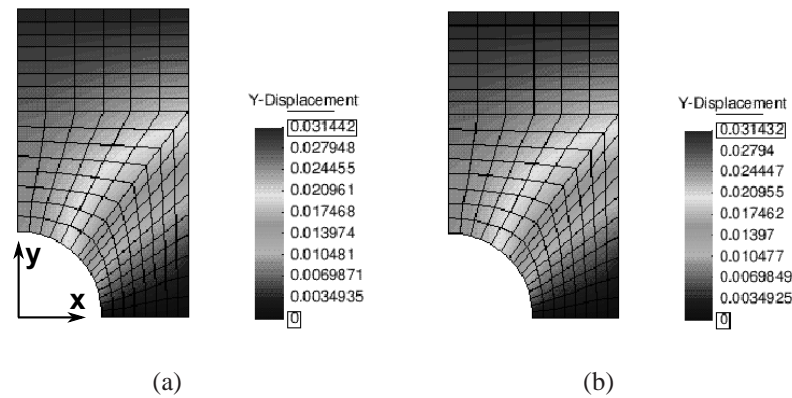


Figure 4.10: Displacements in y direction: (a) conventional material model and (b) PD-NURBS material model.

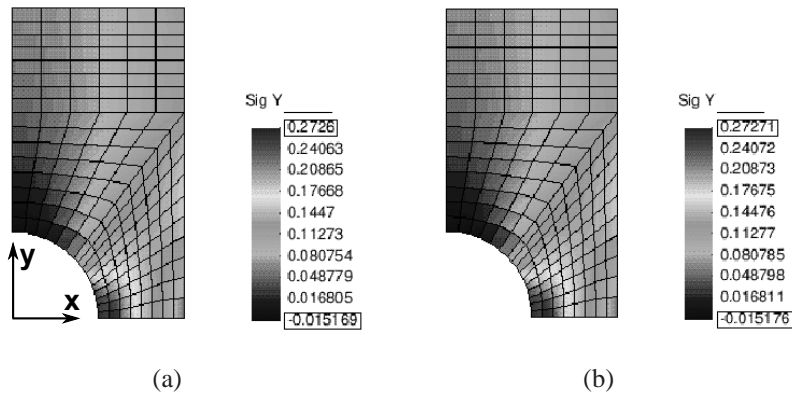


Figure 4.11: Stresses in y direction: (a) conventional material model and (b) PD-NURBS material model.

Table 4.6: Maximum error of the PD-NURBS for perforated membrane

Maximum errors	
displacement y	stress y
0.032%	0.040%

Although the comparison with the elastoplastic models are promising, application of PD-NURBS to path dependent problems requires further investigation.